Materials Research. 2014; 17(6): 1410-1419
DOI: http://dx.doi.org/10.1590/1516-1439.283514

Innovative Low Temperature Plasma Approach for Deposition of Alumina Films

Felipe Augusto Darriba Battaglin[a]*, Ricardo Shindi Hosokawa[a], Nilson Cristino da Cruz[a], Luciano Caseli[b], Elidiane Cipriano Rangel[a], Tiago Fiorini da Silva[c], Manfredo Harri Tabacniks[d]

[a]Laboratório de Plasmas Tecnológicos, Universidade Estadual Paulista – UNESP, Câmpus Experimental de Sorocaba, Avenida Três de Março, 211, Alto da Boa Vista, CEP 18087-180, Sorocaba, SP, Brasil
[b]Departamento de Ciências Exatas e da Terra, Universidade Federal de São Paulo – UNIFESP, Rua Artur Riedel Eldorado, CEP 09972-970, Diadema, SP, Brasil
[c]Departamento de Física Nuclear, Universidade de São Paulo – USP, Rua do Matão, Travessa R, 187, Cidade Universitária, CEP 05508-900, São Paulo, SP, Brasil
[d]Departamento de Física Aplicada, Universidade de São Paulo – USP, Rua do Matão, Travessa R, 187, Cidade Universitária, CEP 05508-900, São Paulo, SP, Brasil

Received: April 13, 2014; Revised: November 17, 2014

Alumina films were deposited from a new plasma method using aluminum acetylacetonate (AAA) powder as precursor. The AAA was sputtered in argon and oxygen plasma mixtures. It was investigated the effect of the oxygen proportion (O_2%) on the properties of the coatings. Deposition rate was derived from the layer height measured by profilometry. The elemental composition and molecular structure of the films were determined by Rutherford backscattering and infrared spectroscopies, respectively. Grazing incidence X-ray diffraction was used to investigate the microstructure of the films while hardness was determined by nanoindentation technique. Inspections on the surface morphology and on the film composition were conducted associating scanning electron microscopy and energy dispersive spectroscopy. Incorporation of oxygen affects the plasma kinetics and consequently the properties of the coatings. As moderated concentrations of oxygen (< 25%) are added, the structure is predominantly organic containing stoichiometric amorphous alumina. On the other hand, as high O_2% (> 25%) are incorporated, the structure become rich in metallic aluminum with carbon rising at low proportions. The deposited layer is not homogeneous in thickness once the chemical composition of the precursor is changed by the action of the reactive oxygen plasma. Oxygen ablation on the film surface also contributes to the lack of homogeneity of the structure, especially as high oxygen proportions are imposed. Hardness data (0.5-2.0 GPa) corroborated the idea of an amorphous structure. Based on the results presented here it was possible to identify the oxygen concentration in the plasma atmosphere which mostly removed organics while preserving the stoichiometric alumina precipitation, subject of great relevance as one considers the reduction in the energy necessary for the creation of fully oxide coatings.

Keywords: *alumina, aluminum acetylacetonate, reactive plasma sputtering, composition, structure, morphology*

1. Introduction

Aluminum oxide, commonly referred to as alumina (Al_2O_3), has interesting properties, such as high thermal insulation, electrical resistivity, hardness, good resistance to wear and corrosion, besides having physical stability at high temperatures[1,2].Owing to that, alumina can be used as abrasives, protective films for optical, electronic and micro-electronic segments, passivation layers, hardener coatings for tools and other applications[3].

Alumina is a polymorphic material being the crystalline alpha (α) phase the responsible for these notorious properties[3]. But the precipitation of the α-Al_2O_3 is complex because its growth is compromised by a large number of existing metastable phases[2,4]. In addition to this fact, the alpha phase is obtained only under high working temperatures. The chemical vapor deposition (CVD) technique commonly, employed to prepare alumina films, requires substrate temperatures of around 1000 °C[1-4]. This fact turns the application of such a coating impractical for materials sensitive to high temperatures[3].

Several techniques using different experimental apparatus have been reported in the literature to obtain amorphous and crystalline alumina films. Carta et al.[3] deposited amorphous alumina coatings on AISI 304 stainless steel substrates by the metal organic chemical vapor deposition (MOCVD) in a hot wall reactor at 380 °C with oxygen in the atmosphere.

*e-mail: darriba@bol.com.br

Another example is showed by Caussat et al.[5], in which SiO_2 powder has been coated by alumina through the fluidized bed chemical vapor deposition process associated with the metal organic precursor, aluminum acetylacetonate ($Al(acac)_3$). The temperature range was 400-620 °C.

Maruyama et al.[6] deposited amorphous alumina films by low-temperature atmospheric-pressure CVD using aluminum acetylacetonate. The precursor, thermally decomposed in air at 150 °C, was carried to the reaction chamber by a nitrogen gas flow, where it was exposed to temperatures ranging from 250 to 600 °C. Authors justify the choice of the AAA by its low toxicity and simplicity of handling.

The same compound was used in the work of Muhsin et al.[7] providing amorphous and crystalline alumina films. As in the Maruyama's[6] work, the precursor was, decomposed at temperatures of around 247 °C and carried to a wall heated-CVD reactor operating at atmospheric pressure. Films deposited at 500 °C were transparent, amorphous and mechanically/chemically stable. Annealing at temperatures higher than 800 °C led to alumina crystallization.

In the work of Jeon et al.[8] amorphous alumina thin films were deposited by the plasma-enhanced atomic-layer deposition (PEALD) method. Two different precursors, dimethylaluminum isopropoxide and trimethylaluminum, were employed associated with the oxygen as the reactant gas in the plasma. Using the filtered vacuum arc method, with a highly pure aluminum cathode and oxygen gas, Yamada-Takamura et al.[1] obtained crystalline and amorphous phases of alumina with a temperature of the substrate between 500-780 °C.

Cibert et al.[9] deposited films by PLD (Pulsed Laser Deposition) and PECVD at room temperature and 800 °C. Trimethylaluminium (TMA), used as the precursor, was admitted to the reaction chamber by a flow of argon passing through it. Amorphous films were found at room temperature, while crystalline ones were obtained at 800 °C.

Kyrylov and co-workers[10] deposited alumina films on molybdenum super alloy and stainless steel substrates from gaseous mixtures ($AlCl_3$, O_2, H_2 and Ar). For that, they used a bipolar mid frequency PECVD system, varying the substrate temperature from 500 to 620 °C. The results revealed that film structure and properties were influenced by the plasma parameters and gas composition. Furthermore, the temperature for the precipitation of the α-alumina (~ 500 °C) was lower than the reported by the CVD method.

Lin and co-workers[11] deposited films on glass and silicon substrates by radio frequency PECVD. The depositing plasmas were generated from $AlCl_3$, CO_2 and H_2 mixtures while heating the sample holder to 300-500 °C. Transparent, colorless and amorphous Al_2O_3 films resulted from all the experiments even with heating of the samples.

Among the processes mentioned above, the PECVD technique has received particular attention due to the possibility of obtaining alumina layers at low temperatures. Owing to this fact, numerous studies have been performed employing this technique. In a recent publication, Nielsen and co-workers[12] proposed a new plasma approach, based in the PECVD apparatus, for depositing amorphous alumina films from aluminum acetylacetonate, a non-toxic, cheap and easy to handle powder normally used for chemical vapor depositions. The novelty of Nielsen's work was to place the AAA powder directly inside a capacitively coupled plasma reactor and to sputter it in argon radiofrequency plasmas. Besides demonstrating the feasibility of the method to prepare amorphous alumina films, it was revealed that film properties, as the proportion of organic contamination, are strongly dependent on the power of the radiofrequency signal employed in the driven electrode.

In this context, the present work aims to study the effect of the plasma chemical composition on the properties of the films produced by this new methodology. Specifically, it is intended to address the effect of oxygen incorporation into argon plasmas, on the properties of the films. Oxygen has a high reactivity towards carbon and may act as an organic scavenger, contributing to the reduction in the energy necessary for formation of fully oxide films. Furthermore, oxygen radicals in the plasma may reduce the activation energy and increase the reaction with the aluminum precursors, thereby favoring the growth of crystalline phases at lower temperatures[5].

2. Experimental

2.1. Deposition procedure

Figure 1 schematically shows the apparatus used for film deposition, following the methodology proposed by Nielsen et al.[12]. Basically, it is composed by a stainless steel reactor containing two parallel plate electrodes (119 mm in diameter, 50 mm apart) inside the reactor. A Tokyo Hy-Power RF-300 radiofrequency power supply (13.56 MHz, 300 W) is connected to one of the electrodes while the remaining one and the chamber walls are earthed.

The system is evacuated by a mechanical rotative pump (Edwards E2M18), being the pressure monitored by a capacitive membrane sensor (Edwards Barocel 600). Gases are introduced in the reactor via stainless steel pipes passing through needles valves (Edwards LV-10K).

Glass, stainless steel and aluminum plates were used as substrates for film deposition. The substrates were first cleaned in ultrasonic baths, according to the procedures described in a previous work[13]. The cleaned samples were attached to the uppermost electrode of the plasma system using adhesive tape and submitted to a plasma ablation procedure to further clean and activate the substrate surfaces. The parameters employed for that are described in Table 1.

To generate the depositing plasmas, 0.8 grams of aluminum acetylacetonate ($C_{15}H_{21}AlO_6$) from Aldrich Chemistry® with 99% purity, was spread directly on the lowermost electrode and not decomposed at high temperature

Table 1. Parameters of the sputtering process.

Sputtering Process	
Chemical composition	**Argon and hydrogen**
Argon / hydrogen proportion	50% / 50%
Gas pressure	1.33 Pa
Time	10 minutes
RF power in the lower electrode	150 W

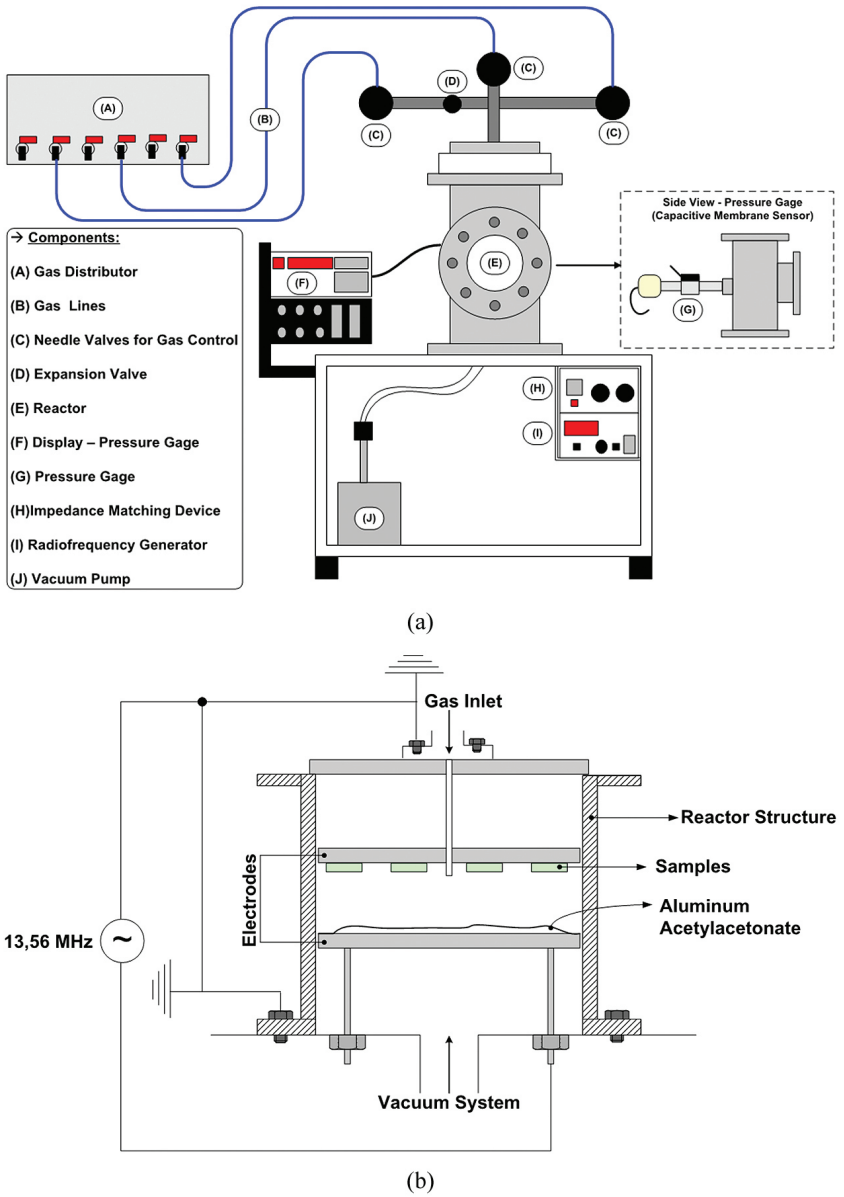

Figure 1. Schematic diagram of the system used for deposition. (a) General. (b) Electrical.

for vapor generation, as demonstrated in previous works that used the PECVD technique with acetylacetonate. The system was pumped down to achieve the base pressure of 4.3 Pa. Argon and oxygen mixtures were admitted in the reactor raising the system pressure to 11 Pa; thereby the gas pressure (oxygen and argon) used was 6.7 Pa. The plasma was ignited by the application of radiofrequency power (13.56 MHz, 150 W) to the lowermost electrode containing the powder of AAA, while grounding the sample holder and the chamber walls. Eight different depositions were conducted changing, from run to run, the acetylacetonate powder and varying the chemical composition of the plasma atmosphere. For that, the proportion of oxygen was increased in the gas mixture from 0 to 100% while that of argon was proportionally decreased to keep the total gas pressure constant in 11 Pa. The respective gas flow added for each deposition cycle is shown in Table 2. Deposition time was 5400 s.

The temperature was measured by a digital thermometer directly on the lowermost electrode, shortly after opening the reactor. The temperature did not exceed 60 °C, value close to that found by Nielsen et al.[12].

2.2. Film characterization

Thickness of the films was measured in samples prepared on glass plates with a step delineated during film deposition. For that, part of the glass surface was masked with a plasma resistant Kapton tape (3M 5413) and exposed to the deposition procedure. After deposition, the Kapton mask was removed revealing the step between

the exposed and protected regions. The height of the step was determined with the aid of a Dektak 150 profilemeter at six different positions of the sample. The analysis was performed considering scans of 200 μm and under a tip load of 3.0 mg. Deposition rate was evaluated as the ratio between film thickness and deposition time.

The average roughness of the samples prepared on glass plates was derived from topographic profiles acquired by profilometry, in the same device used for thickness measurements. For the calculations, three scans of 200 μm were taken from different points of each sample using a tip load of 3.0 mg.

The elemental composition of the films prepared on stainless steel or on aluminum plates were inspected simultaneously by Rutherford Backscattering Spectroscopy (RBS) and Forward Recoil Spectroscopy (FRS) at LAMFI-USP using 2.4 MeV He^{++} particles. The beam incidence angle was 80°, the detector for RBS measurements was placed at 170° scattering angle and for FRS 20° scattering angle (and with a 6-μm thick aluminum filter) referred to the beam direction. From the simulation of the spectra with the SIMNRA code[14], the concentration of the sample species was obtained.

Infrared reflectance absorbance spectroscopy was employed to investigate the molecular structure of the films in a Jasco FTIR-410 spectrometer. The spectra, collected from samples deposited on polished stainless steel substrates, correspond to the average between 128 scans with 4 cm^{-1} of resolution. In addition, Polarization-Modulation Infrared Reflection Absorption Spectroscopy, PM-IRRAS, was employed to inspect the film surface. A KSV PMI 550 Instrument spectrometer was used for that.

To evaluate if there was precipitation of crystalline phases of alumina in the films, grazing incidence X-ray diffraction (GXRD) experiments were conducted in samples deposited on amorphous glass plates. The measurements were performed in a Panalytical X'Pert Powder XRD-6000 diffractometer using a Cu K-alpha (40 kV, 30 mA) radiation source and varying the scanning detector angle from 20 to 90° at a rate of 10.5°/min. Incidence angle was 1°.

Inspections on the surface morphology and elemental composition of the samples prepared on 304 stainless steel plates were conducted associating scanning electron microscopy (SEM) and energy dispersive spectroscopy (EDS). The analyses were accomplished in a Jeol JSM-6010LA (Analytical Scanning Electron Microscope) equipment using secondary electrons detector with beam energy of 2.5 kV (spot size 3 nm and penetration depth around 150 nm).

Hardness was determined from samples prepared on glass plates in a nanoindenter Hysitron Triboindenter. A pyramidal Berkovich tip was employed using a multiple step partial unload trapezoidal function. In this function, the maximum load was varied from 80 to 1000 μN in ten steps while the application, removal and dwell times were fixed in 1s. The results, obtained using the Oliver and Pharr method[15], correspond to the average of 15 indentations conducted for each one of the ten applied force.

3. Results and Discussion

Figure 2 shows the deposition rate of the films as a function of the oxygen concentration in the plasma. Deposition rate firstly increases (7.8 to 25.2 nm/min) as O_2% is elevated from 0 to 20%, suddenly falls (0.59 nm/min) as 25% of oxygen is present, keeping roughly constant with increasing O_2% beyond 25%. Interestingly, a behavior very similar to that was reported in the work of Lin et al.[11] with changing the radiofrequency power employed to the sample holder to excite plasmas from $AlCl_3$, CO_2 and H_2 mixtures. A maximum in deposition rate was reached as power was increased to 200 W followed by a sudden drop with further increasing power. These results were ascribed to changes

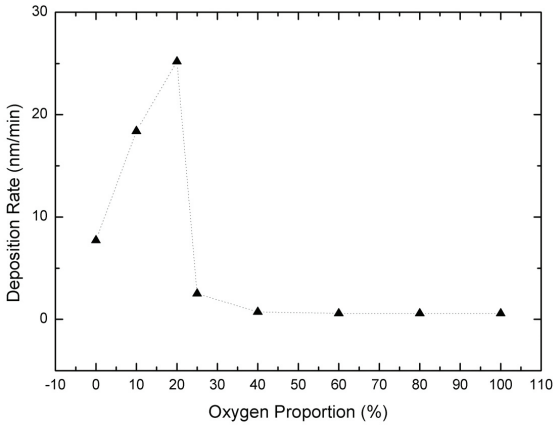

Figure 2. Deposition rate as a function of the oxygen concentration in the plasma.

Table 2. Proportions of oxygen-argon and gas flow employed in each one of the 8 deposition cycles.

Deposition Cycles			
Oxygen proportion [%]	**Oxygen flow [sccm]**	**Argon proportion [%]**	**Argon flow [sccm]**
0	0	100	9.21
10	1.83	90	8.20
20	2.16	80	7.53
25	2.25	75	7.00
40	2.83	60	6.01
60	3.51	40	4.52
80	4.65	20	2.80
100	5.70	0	0

in the plasma kinetics and in the self bias voltage with increasing the excitation power.

In the work of Nielsen et al.[12], deposition rates from 0.1 to 81.3 nm/min were obtained with changing the plasma excitation power from 50 to 300 W but with no oxygen incorporation. Considering oxygen addition, it clearly accelerates deposition rate as moderate proportions (20%) are used. Once sputtered to the plasma phase, AAA molecules or fragments can be further activated prior deposition, enhancing the overall plasma reactivity. Since oxygen has a high affinity towards the organic part of the AAA, activation is more prone to occur as oxygen is present in the plasma. Furthermore, the interaction of atomic oxygen with the deposited film may also generate active sites for film deposition. That is, oxygen favors the activation of the plasma and of the film species, both accelerating the deposition process.

However, as oxygen proportion exceeds 20%, there is alteration in the deposition-removal balance due to changes promoted in three phenomena. Firstly, the ejection of AAA constituents to the plasma by sputtering is substantially reduced since O atoms are lighter than Ar ones. Secondly, the removal of newly deposited species from the substrate surface by the etching process rises[16]. Finally, there is a higher probability of oxidizing the aluminum part of the molecule in the plasma phase, then reducing the availability of reactive aluminum precursors for film formation since oxide groups are very stable.

Aside to these effects, the chemical composition of the precursor may also be changed as oxygen is incorporated. The affinity of oxygen towards carbon and hydrogen tends to preferentially remove organics from the AAA powder, turning more inorganic the remaining precursor in the reactor. During the first stages of the deposition process the etched organic functionals can be activated in the plasma phase and incorporated in the film structure, however, in the final stages they are no longer abundant in the depositing atmosphere, resulting in a gradient layer in which the inorganic fraction grows from the substrate to the surface.

The elemental composition of the films, derived from the RBS results, is presented as a function of O_2% in Figure 3. For the films deposited with 0 to 20% of oxygen in the plasma, C, O and H are the prominent species in the structure with aluminum rising in smaller concentrations (ten times lower). While the proportions of the first three elements are observed to linearly fall with increasing O_2% up to 20%, the proportion of Al keeps roughly constant. Interestingly, as 25% of oxygen is incorporated in the plasma phase, the concentrations of Al and O in the structure grow. For higher oxygen proportions (> 25%) the concentration of carbon atoms is reduced (~ 2 orders of magnitude) while that of Al increases, becoming the prominent species in the structure. In this case, oxygen and hydrogen concentrations assume intermediary position between that of Al and C. The dotted vertical line in the graph represents the transition from a structure with excess of carbon to another with excess of Al, showing that oxygen incorporation in the plasma phase indeed acts as a carbon scavenger but when in excess (> 25%) tends to result in metallic aluminum films. The Al/O ratio intensity, depicted in Figure 4, clearly demonstrates such a transition.

Furthermore, as the availability of reactive oxygen in the plasma grows the etching of organics from the newly deposited surface also increases, further contributing to originate a gradient structure with abundance of Al in uppermost interface. Indeed the roughly constant carbon concentration in the films even with the increment in O_2% may be a result of the stronger C incorporation during the first stages of the deposition process.

The infrared spectra of the films deposited on polished 304 stainless steel, using 0, 10 and 20% of oxygen in the plasma, are shown in Figure 5. The absorptions detected in these spectra were collected and identified in Table 3. All the other samples resulted in featureless spectra due to the low amount of deposited material associated to the high fraction of metallic aluminum in the structure.

Bands related to stretching (2876, 2933 and 2966 cm^{-1})[12] and bending (1464, 1403 and 1293 cm^{-1})[12] vibrations of C-H groups were detected altogether with those ascribed to stretching (~3447 cm^{-1}) modes of O-H groups[6]. Carbonyls (C=O) are also identified by the absorptions around 1704[12] and 1596[17] cm^{-1}. As connected to aluminum groups, such bands emerge at 1531[12] cm^{-1}.

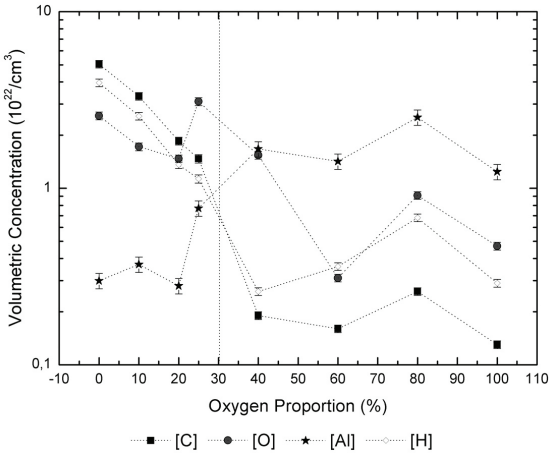

Figure 3. Concentrations of C, H, O and Al of the films as a function of O_2%.

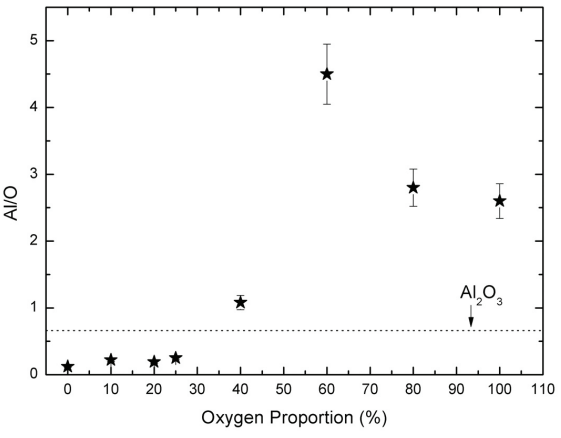

Figure 4. Al/O intensity ratio as a function of O_2%.

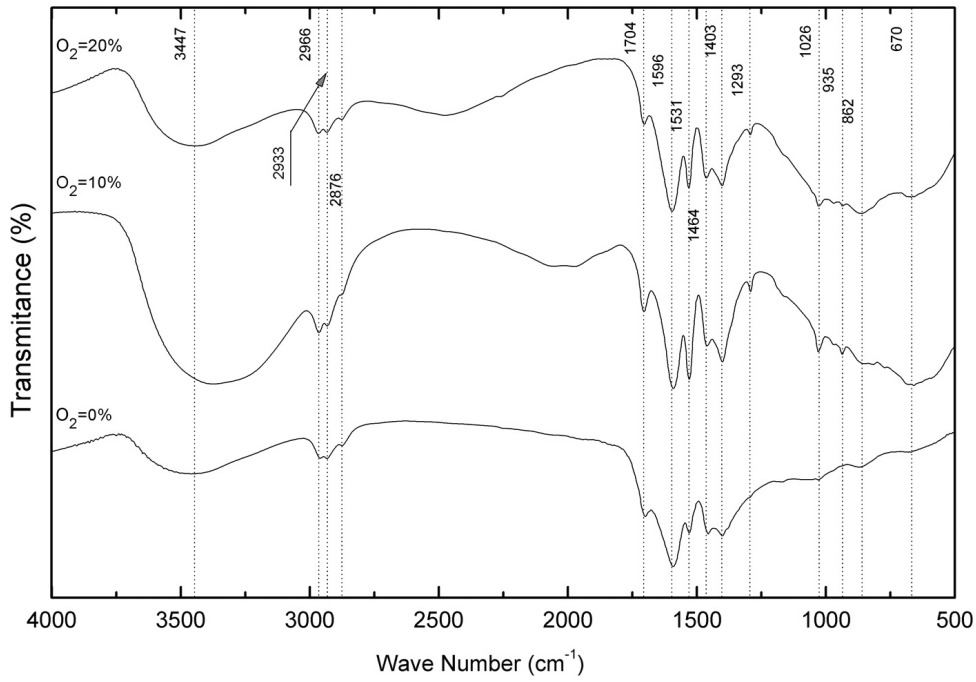

Figure 5. Reflectance-absorbance infrared spectra of the films deposited with different oxygen concentrations in the plasma.

Table 3. Wavenumber of the absorption bands present in the infrared spectra of the films and their respective assignments.

Wavenumber [cm^{-1}]	Assignment
3447	ν O-H
2966	ν C-H
2933	ν C-H
2876	ν C-H
1704	C=C
1596	ν C=O
1531	ν C=O connected to aluminum
1464	δ C-H
1403	δ C-H
1293	δ C-H
1026	ν Al=O
935	LO Al_2O_3
862	ν Al-O
670	TO Al_2O_3

In the low wavenumber region of the spectra (500 – 1200 cm^{-1})[6], the presence of aluminum is detected by the absorptions at 1026 (ν Al=O)[12], 935 (LO Al_2O_3)[1], 862 (ν Al-O)[12] and 670 (TO Al_2O_3)[1] cm^{-1}, overlapped to a large and intense contribution ranging from 500 to 1200 cm^{-1}, characteristic of amorphous alumina[1]. Even as oxygen is incorporated at low concentrations (10%), the intensity of the bands related to the amorphous alumina (≤ 1000 cm^{-1})[1] becomes more prominent than that observed for the organic ones (1250-2000 cm^{-1})[12].

The polarization modulation infrared spectra of the samples, acquired in the 800 to 1200 cm^{-1} region, are presented in Figure 6. They represent the difference between the signal taken from the bare glass substrate (background)

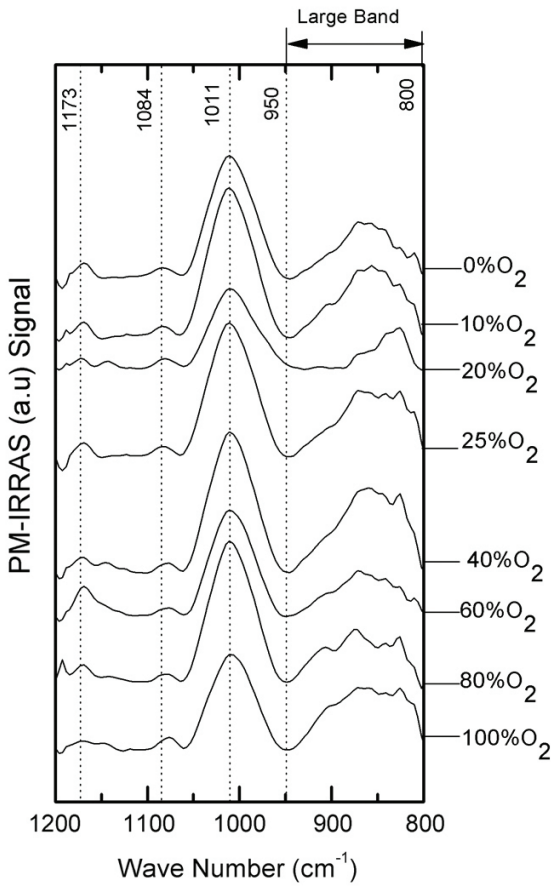

Figure 6. PM-IRRAS spectra for the films deposited using different oxygen proportions in plasma.

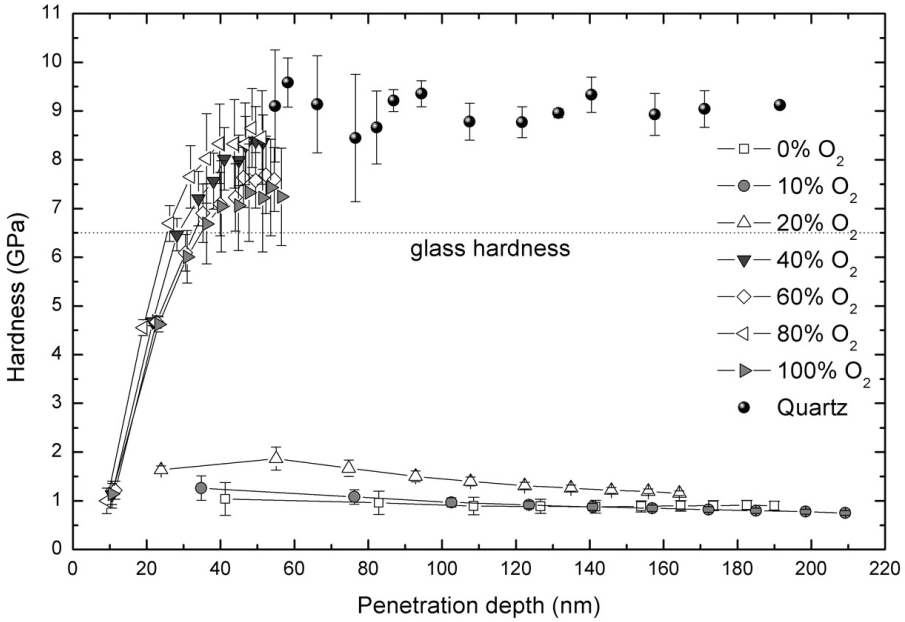

Figure 7. Hardness of the films as a function of the penetration depth of the diamond tip.

and the film containing glass. The wavenumbers and respective assignments of all contributions were collected in Table 4. The most prominent contribution in the spectra, emerging at 1011 cm^{-1}, is characteristic of the stretching vibration of Al=O groups[12]. Further indication of Al incorporation is provided by the large contribution in the 800 to 950 cm^{-1} region, which may originate from amorphous alumina[12] and/or from Al-O[17] (860 cm^{-1}) stretching vibrations. Maruyama et al.[6] also verified the rise of a broad band lying from 500 to 1000 cm^{-1} in the infrared spectra of the films which was attributed to vibrations of Al_2O_3 groups. These two stronger absorptions are similar for all the samples, showing no dependency on the oxygen proportion. Aside to these, lower intensity contributions, created from deformations of O-H groups and O-H connected to the Al_2O_3 structure[18], are evidenced around 1173 and 1084 cm^{-1}, respectively. Incorporation of hydroxyl groups in alpha alumina was also reported by Giner et al.[19] in the same region and using the same analysis.

Therefore, regardless the oxygen proportion which was employed, the spectra presented in Figure 6 reflect surfaces with the same molecular structure unless for slight changes. This result is ascribed to the depletion of organics from the film surfaces caused by the plasma ablation as well as to the inorganic nature of the AAA in the final stages of the deposition.

The creation of an amorphous structure is further confirmed as one considers the GXRD results of the films (not shown). This result is coherent with the previous work of Nielsen et al.[12] as well as with other reports in the literature[20], in which amorphous alumina films were derived from low temperature plasma depositions. According to estimations[20], the sample holder does not reach 100 °C under the conditions employed here.

Figure 7 shows the hardness of the films as a function of the penetration depth of the diamond tip. Hardness values for the standard quartz plate (9.0 GPa), also presented in this graph, were used to calibrate the indenter tip area. For the thinnest films (O_2% > 20%) no conclusive results are obtained since the tip senses the underlying glass substrate (6-7 GPa). On the other hand, for the thickest layers (O_2% < 20%), almost straight lines, lying between

Table 4. Wavenumber of the absorption bands and assignment present in the PM-IRRAS spectra.

Wavenumber [cm^{-1}]	Assignment
1173	**Deformations of O-H groups**
1084	**O-H connected to the Al_2O_3**
1011	**ν Al=O**
950 to 800	Amorphous alumina and/or ν Al-O (860 cm^{-1})

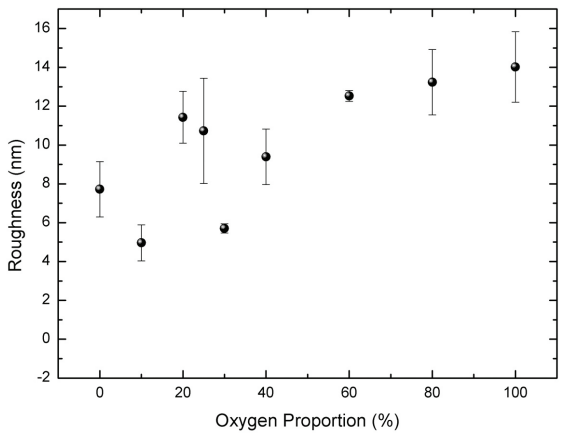

Figure 8. Roughness of the films deposited on glass substrates as a function of the oxygen concentration in the plasma

0.5 and 2.0 GPa, are obtained for the substrate interference free region (< 100 nm). For 0 and 10% of oxygen, values commonly found in plasma deposited organic materials (~1.0 GPa) are measured in good agreement with the results reported by Nielsen and co-workers[12]. Hardness increases about twice (~ 2.0 GPa) as 20% of oxygen was employed for film deposition, corroborating the previous interpretation of an amorphous oxide-richer structure for this sample.

Figure 8 shows the average roughness, Ra, of the films as a function of O_2%. Despite some oscillations, a rise trend is observed with increasing the oxygen concentration in the plasma phase. Ra values between 5 and 11 nm were found as O_2% was changed from 0 to 25%. These results are slightly higher than the reported by Cibert and co-workers[9] for the roughness of alumina films deposited at room temperature on silicon substrates using the PECVD technique. The rising trend in Ra is ascribed to two primary effects. First of all, the interaction of reactive oxygen groups with the surface generates defects on the growing layer elevating the number of active sites for film growth. Furthermore, the abundance of oxygen during the depositions also promotes the removal of species from the surface through the etching process[16]. Both phenomena contribute to defect generation justifying the roughness increment.

Figure 9 shows the scanning electron micrographs and EDS spectra of the samples deposited on polished stainless steel substrates. The same results for the bare substrate, presented in Figure 9(a), reveal a flat surface containing

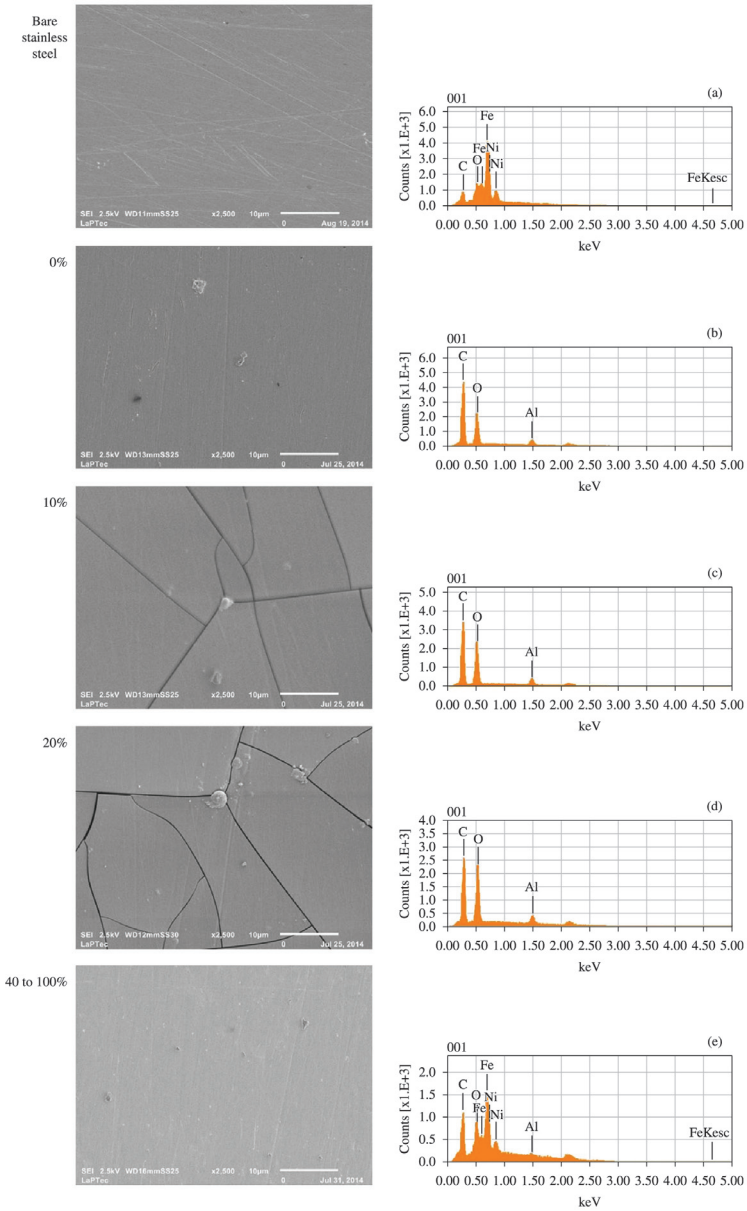

Figure 9. Secondary electron micrographs (beam energy of 2.5 kV, spot size 3 nm and penetration depth around 150 nm) and EDS spectra of the (a) bare stainless steel substrate and of the films deposited with (b) 0%, (c) 10%, (d) 20% and (e) 40 -100% of oxygen in the plasma.

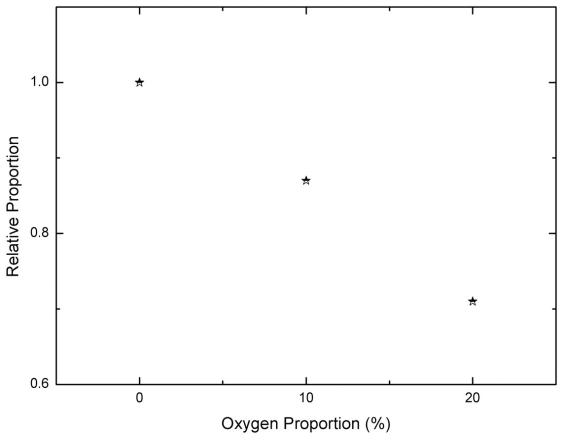

Figure 10. C/Al intensity ratio obtained from the EDS peaks for samples where the film was detected.

scratches and the common elements found in this alloy (C, Cr, Ni, Si, Mn, P and S)[21]. After submission to the depositing plasma (O_2% = 0), the surface morphology slightly changes with the disappearance of the scratches present in the metallic surface. The presence of a uniform coating is readily confirmed by detection of C, Al and O and by disappearance of the alloying elements in the EDS spectrum of this sample. As oxygen is incorporated in the plasma (up to 20%), there is rise of cracks over the entire surface. The same phenomenon was observed in the work of Nielsen et al.[12] as film thickness reached around 2 µm, being associated to the fragile nature of the oxide films and to the elevation in the internal stress promoted by the thickness enhancement. Carbon, oxygen and aluminum are still detected on the cracked surface. The C/Al intensity ratio, evaluated from the EDS peaks and presented in Figure 10, clearly shows a fall trend then confirming the effect of O on the organic components[12]. Consistently with the increment in the film thickness, the intensity of the peaks ascribed to alloying elements vanishes in the EDS spectra. Finally, with increasing oxygen concentration beyond 20%, a surface with no cracks and relatively uniform develops, indicating that plasma process affects in a lower extent the surface morphology. The film elements are barely detected by the EDS analysis due the penetration depth of the probing electron beam. Further indication of changes is obtained from the morphology of these samples which present a higher uniformity than the observed in the bare substrate. In general, the analysis derived from SEM and EDS data are in good agreement with those established from RBS and infrared results.

4. Conclusions

Films were deposited from the reactive sputtering of aluminum acetylacetonate in argon and oxygen plasma mixtures. The proportion of oxygen incorporated was observed to affect the plasma kinetics. Deposition rate is influenced by the oxygen addition since it reduces the sputtering of AAA, increases the ablation of the deposited material and decreases the content of reactive aluminum available in the plasma for deposition. Chemical changes are also expected in the precursor and on the growing layer due to the action of the plasma atmosphere affecting the overall morphology and roughness of the surfaces.

It was clearly identified a transition from a regime in which oxygen addition scavenges the organic part of the structure to another one that results in predominantly metallic films. Amorphous alumina was detected in the bulk and on the surface of the films being their proportions dependent on O_2%. Films are amorphous since the deposition proceeded at temperatures lower than 100 °C. The thickest films containing high proportions of alumina cracked; lower deposition times are proposed to reduce the layer thickness while preserving higher oxides proportions. Hardness results are consistent with the amorphous nature of films and also with the presence of organics in deeper regions of the coatings.

Considering all these results, the optimum proportion of oxygen in the plasma was considered to be 25% since it promoted the lowest C content while preserving the oxide nature of the coating. For this condition, Al/O ratio was the closest to that of alumina and no cracks were detected in the film structure, a positive point as one considers practical applications. The study conducted here was of substantial importance since it will enable a reduction in the energy necessary to formation of fully oxide coatings using this new methodology. For that, it is proposed to associate resistive heating or ion bombardment, recognized carbon scavenger methods, to the reactive sputtering of the AAA.

Acknowledgements

The authors would like to acknowledge FAPESP (Fundação de Amparo à Pesquisa do Estado de São Paulo) for financial support (2009/07604-3 and 2012/14708-2).

References

1. Yamada-Takamura Y, Koch F, Maier H and Bolt H. Characterization of α-phase aluminum oxide films deposited by filtered vacuum arc. *Surface and Coatings Technology*. 2001; 142-144:260-264. http://dx.doi.org/10.1016/S0257-8972(01)01206-3.
2. Wallin E. *Alumina thin film growth: experiments and modeling*. [Dissertation]. Linköping: Linköping University; 2007.
3. Carta G, Natali M, Rigato V, Rossetto G, Salmaso G and Zanella P. Chemical, morphological and nano-mechanical characterizations of Al2O3 thin films deposited by metal organic chemical vapour deposition on AISI 304 stainless steel. *Electrochimica Acta*. 2005; 50(23):4615-4620. http://dx.doi.org/10.1016/j.electacta.2004.10.097.
4. Sarakinos K, Music D, Nahif F, Jiang K, Braun A, Zilkens C, et al. Ionized physical vapor deposited Al2O3 films: does subplantation favor formation of α-Al2O3? *Physica Status Solidi (RRL): Rapid Research Letters*. 2010; 4(7):154-156. http://dx.doi.org/10.1002/pssr.201004133.
5. Caussat B, Rodriguez P, Iltis X, Ablitzer C and Brothier M. Alumina coatings on silica powders by fluidized bed chemical

vapor deposition from aluminum acetylacetonate. *Chemical Engineering Journal*. 2012; 211-212:68-76. http://dx.doi.org/10.1016/j.cej.2012.09.048.

6. Maruyama T and Arai S. Aluminum oxide thin films prepared by chemical vapor deposition from aluminum acetylacetonate. *Applied Physics Letters*. 1992; 60(3):322-323. http://dx.doi.org/10.1063/1.106699.
7. Muhsin AE. *Chemical vapor deposition of aluminum oxide (Al2O3) and beta iron disilicide (β-FeSi2) thin films*. [Dissertation]. Essen: Universität Duisburg; 2007.
8. Jeon S, Jeon H Koo J and Kim S,. Characteristics of Al2O3 thin films deposited using dimethylaluminum isopropoxide and trimethylaluminum precursors by the plasma-enhanced-atomic-layer deposition method. *Journal of the Korean Physical Society*. 2006; 48(1):131-136.
9. Cibert C, Hidalgo H, Champeaux C, Tristant P, Tixier C, Desmaison J, et al. Properties of aluminum oxide thin films deposited by pulsed laser deposition and plasma enhanced chemical vapor deposition. *Thin Solid Films*. 2008; 516(6):1290-1296. http://dx.doi.org/10.1016/j.tsf.2007.05.064.
10. Kyrylov O, Cremer R and Neuschutz D. Deposition of alumina hard coatings by bipolar pulsed PECVD. *Surface and Coatings Technology*. 2003; 163-164:203-207. http://dx.doi.org/10.1016/S0257-8972(02)00482-6.
11. Lin CH, Wang HL and Hon MH. Preparation and characterization of aluminum oxide films by plasma enhanced chemical vapor deposition. *Surface and Coatings Technology*. 1997; 90(1-2):102-106. http://dx.doi.org/10.1016/S0257-8972(96)03100-3.
12. Nielsen GF. *Filmes orgânicos contendo óxido de alumínio depositados a plasma*. [Dissertation]. Sorocaba: Universidade Estadual Paulista; 2011.
13. Mancini SD, Nogueira AR, Rangel EC and Cruz NC. Solid-state hydrolysis of post consumer polyethylene terephthalate after plasma treatment. *Journal of Applied Polymer Science*. 2013; 127(3):1989-1996. http://dx.doi.org/10.1002/app.37591.
14. Mayer M. SIMNRA: a Simulation Program for the Analysis of NRA, RBS and ERDA. In: Proceedings of the 15th International Conference on the Application of Accelerators in Research and Industry; 1999; Denton. American Institute of Physics Conference Proceedings; 1999. p. 541.. http://dx.doi.org/10.1063/1.59188.
15. Li H and Vlassak JJ. Determining the elastic modulus and hardness of an ultra-thin film on a substrate using nanoindentation. *Journal of Materials Research*. 2009; 24(03):1114-1126. http://dx.doi.org/10.1557/jmr.2009.0144.
16. Sant'Ana PL. *Tratamento a plasma de polímeros comerciais transparentes*. [*Dissertation*]. Sorocaba: Universidade Estadual Paulista; 2010.
17. Nielsen GF, Silva LHF, Cruz NC and Rangel EC. Preparation of films from aluminum acetylacetonate by plasma sputtering. *Surface and Interface Analysis*. 2013; 45(7):1113-1118. http://dx.doi.org/10.1002/sia.5236.
18. Thissen P, Wielant J, Köyer M, Toews S and Grundmeier G. Formation and stability of organophosphonic acid monolayers on ZnAl alloy coatings. *Surface and Coatings Technology*. 2010; 204(21-22):3578-3584. http://dx.doi.org/10.1016/j.surfcoat.2010.04.027.
19. Giner I, Maxisch M, Kunze C and Grundmeier G. Combined in situ PM-IRRAS/QCM studies of water adsorption on plasma modified aluminum oxide/aluminum substrates. *Applied Surface Science*. 2013; 283:145-153. http://dx.doi.org/10.1016/j.apsusc.2013.06.059.
20. Chryssou CE and Pitt CW. 2O3 thin films by plasma-enhanced chemical vapour deposition using trimethyl-amine alane (TMAA) as the Al precursor. *Applied Physics. A, Materials Science & Processing*. 1997; 65(4-5):469-475. http://dx.doi.org/10.1007/s003390050611.
21. Zaika AC. *Propriedades Mecânicas e tribológicas de aço austenítico 304 submetido à nitretação por: implantação iônica e implantação iônica por imersão em plasma.* [Dissertation]. Ponta Grossa: Universidade Estadual de Ponta Grossa; 2007.